THE JOURNAL OF PHYSICAL CHEMISTRY A

Article

pubs.acs.org/JPCA

Gas-Phase Synthesis of Boronylallene ($H_2CCCH(BO)$) under Single Collision Conditions: A Crossed Molecular Beams and Computational Study

Surajit Maity, Dorian S. N. Parker, and Ralf I. Kaiser*

Department of Chemistry, University of Hawaii at Manoa, Honolulu, Hawaii 96822, United States

Brad Ganoe, Stefan Fau, Ajith Perera, and Rodney J. Bartlett*

Quantum Theory Project, University of Florida, Gainesville, Florida 32611, United States

Supporting Information

ABSTRACT: The gas phase reaction between the boron monoxide radical (^{11}BO; $X^2\Sigma^+$) and allene (H_2CCCH_2; X^1A_1) was investigated experimentally under single collision conditions using the crossed molecular beam technique and theoretically exploiting *ab initio* electronic structure and statistical (RRKM) calculations. The reaction was found to follow indirect (complex forming) scattering dynamics and proceeded via the formation of a van der Waals complex ($^{11}BOC_3H_4$). This complex isomerized via addition of the boron monoxide radical (^{11}BO; $X^2\Sigma^+$) with the radical center located at the boron atom to the terminal carbon atom of the allene molecule forming a $H_2CCCH_2{}^{11}BO$ intermediate on the doublet surface. The chemically activated $H_2CCCH_2{}^{11}BO$ intermediate underwent unimolecular decomposition via atomic hydrogen elimination from the terminal carbon atom holding the boronyl group through a tight exit transition state to synthesize the boronylallene product ($H_2CCCH^{11}BO$) in a slightly exoergic reaction (55 ± 11 kJ mol^{-1}). Statistical (RRKM) calculations suggest that minor reaction channels lead to the products 3-propynyloxoborane ($CH_2(^{11}BO)CCH$) and 1-propynyloxoborane ($CH_3CC^{11}BO$) with fractions of 1.5% and 0.2%, respectively. The title reaction was also compared with the cyano (CN; $X^2\Sigma^+$)−allene and boronyl−methylacetylene reactions to probe similarities, but also differences of these isoelectronic systems. Our investigation presents a novel gas phase synthesis and characterization of a hitherto elusive organyloxoborane (RBO) monomer—boronylallene—which is inherently tricky to isolate in the condensed phase except in matrix studies; our work further demonstrates that the crossed molecular beams approach presents a useful tool in investigating the chemistry and synthesis of highly reactive organyloxoboranes.

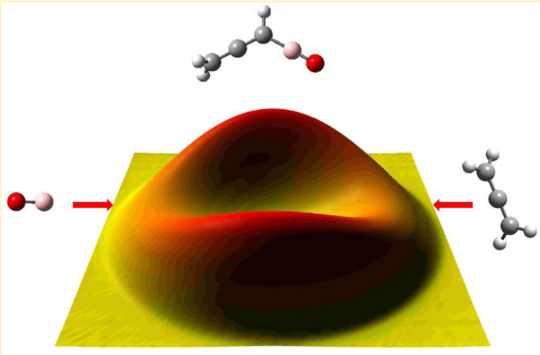

1. INTRODUCTION

In recent years, boronic acids ($RB(OH)_2$) and their derivatives have emerged as crucial reagents in modern organic synthesis[1−7] acting as molecular building blocks in crystal engineering.[8−10] Suginome et al. exploited boronic acid derivatives to synthesize sequences of oligoarenes using Suzuki−Miyaura cross-coupling reactions.[1−4] Further, Hall et al. probed regioselective and stereoselective reactions using boronic acid derivatives.[5−7] The characterization of boronic acid derivatives and their reactions were discussed elaborately by Hall.[11] Compared to boronic acid derivatives, the anhydrides of boronic acid—organyloxoboranes (RBO; R = organyl)—have remained less explored. Recently, the synthesis and characterizations of organyloxoboranes have attracted researchers due to the presence of strong boron−oxygen multiple bonds.[12,13] Early studies of oxoborane utilizing microwave and infrared spectroscopy have proposed the evidence of a very strong boron−oxygen triple bond.[14−16] However, oxoboranes are very reactive due to the highly polar boron−oxygen bond and readily form oligomers to compensate for their intrinsic electron deficiency.[17,18] As a result, the dehydration of boronic acids lead to the formation of oligomers of oxoborane instead of monomers.[17] Further, Bock et al. reported the synthesis of methyloxoborane (CH_3BO) via thermolysis of methyl-1,3,2-diborolane-4,5-dione, but the product promptly underwent cyclo-oligomerization to $(CH_3BO)_3$.[19] The cyclo-oligomerization of RBO can be observed even at temperatures as low as 50 K;[17] isolated oxoboranes were reported either as reactive intermediates or in cryogenic matrices.[15,19,20] For example, Andrews et al. detected methyloxoborane (CH_3BO) and methyleneoxoborane (CH_2BO) while studying reactions of laser-ablated boron atoms with methanol in a low-temperature

Received: February 13, 2014
Revised: April 30, 2014

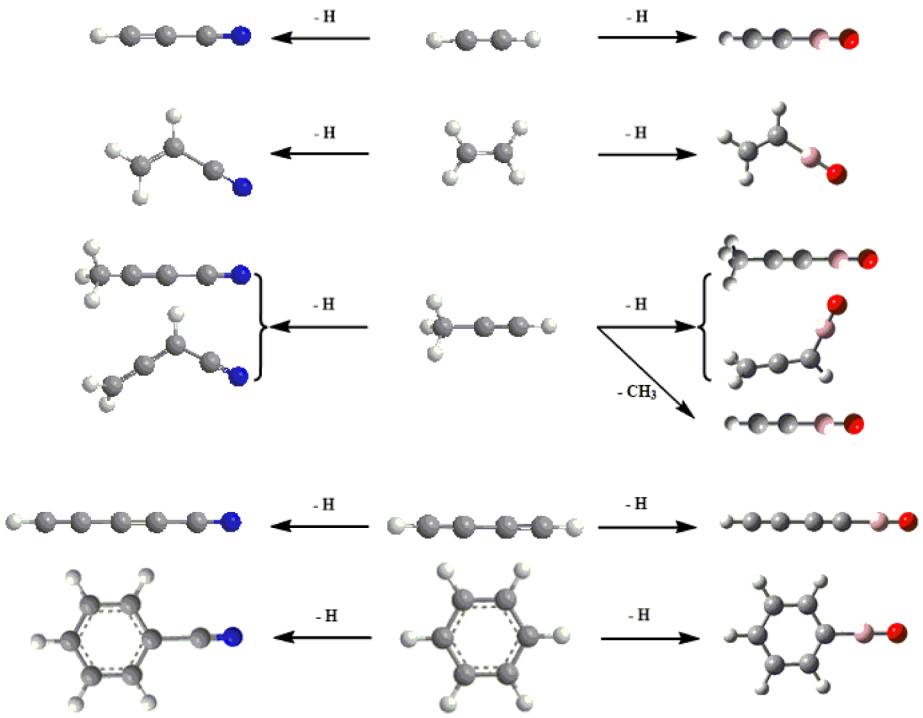

Figure 1. Reactive scattering products detected previously in the gas phase under single collision conditions via the reaction of isoelectronic (left-hand side) cyano (CN; $X^2\Sigma^+$) radical[34−36,38−40] and (right-hand side) boron monoxide (BO; $X^2\Sigma^+$) radical[25−29] with unsaturated hydrocarbon (center).

argon matrices.[15] Recently, Braunschweig et al. synthesized a stable oxoboryl complex, $(Cy_3P)_2Pt(BO)Br$ (Cy = cyclohexyl), for the first time.[21,22] However, experimental evidence of stable oxoboranes is still sparse, and limited theoretical investigations exist.[23,24] The gas phase synthesis of oxoboranes can lead to the formation of a stable molecule but has never been explored except in recent crossed molecular beam experiments probing the reactions of boron monoxide radicals with unsaturated hydrocarbons in our group.[25−29] These studies revealed the formation of ethynyloxoborane (HCCBO), ethenyloxoborane (H_2CCHBO), 1-propynyloxoborane (CH_3CCBO), butadiynyloxoborane (HCCCCBO), and phenyloxoborane (C_6H_5BO) in gas phase reactions with acetylene, ethylene, methylacetylene, diacetylene, and benzene.[25−29]

A recent theoretical study on the oxoboryl (BO)-substituted acetylene[30] revealed that this system is comparable to isoelectronic cyano-substituted hydrocarbons; this study found that the oxoboryl (BO) group serves as a sigma radical in this covalent system similar to the nitrile (CN) group in substituted hydrocarbons. Further, the boron monoxide radical (BO; $X^2\Sigma^+$) and the cyano radical (CN; $X^2\Sigma^+$) are isoelectronic.[31−33] Therefore, both the reactions of $BO(X^2\Sigma^+)$ and $CN(X^2\Sigma^+)$ with unsaturated hydrocarbon molecules are expected to hold similar reaction mechanisms. Note that the bimolecular reaction of the cyano radical with hydrocarbons such as acetylene (C_2H_2),[34] ethylene (C_2H_4),[35] methylacetylene (CH_3CCH),[36] allene (H_2CCCH_2),[36] propylene (CH_3CHCH_2),[37] dimethylacetylene (CH_3CCCH_3),[38] diacetylene (C_4H_2),[39] and benzene (C_6H_6)[40] was explored experimentally and theoretically to unravel the fundamental reaction mechanisms and chemical bonding in the final reaction products together with their thermodynamic properties (enthalpies of formation). These reactions were conducted in the gas phase under single collision conditions utilizing a crossed molecular beam machine; here, the nascent reaction products were formed without "alteration" from wall effects and/or subsequent reactions. In the cyano radical reactions, the cyano radical was found to add with its radical center located on the carbon atom to the sterically least hindered carbon atom of the hydrocarbon molecule without an entrance barrier. The resulting collisional complex underwent unimolecular decomposition—mainly via atomic hydrogen loss—ultimately yielding nitriles (RCN) such as cyanoacetylene (HCCCN), vinyl cyanide (C_2H_3CN), and cyanomethylacetylene (CH_3CCCN) in overall exoergic reactions (Figure 1).[41] Recent crossed beam studies of the reactions of boron monoxide radical with hydrocarbons (acetylene, ethylene, methylacetylene, diacetylene, benzene) have shown excellent similarities (Figure 1) with the reactions of cyano radicals with hydrocarbons such as the reaction mechanism (indirect reaction mechanism via complex formation),[25−29] addition with the radical center located at the boron and carbon atoms to the unsaturated hydrocarbon, decomposition via tight exit transition states through hydrogen loss, and overall exoergic pathways.

Here, we are expanding these studies and probe the reaction of the boron monoxide radical with allene (H_2CCCH_2) to elucidate the reaction mechanism and dynamics of the formation of organyloxoborane under single collision reaction conditions. Allene (CH_2CCH_2) is the simplest cumulene with three carbon atoms connected via two carbon−carbon double bonds which make it more reactive than the corresponding alkenes. By investigating the reaction mechanism of the formation of small boronyl-bearing organic molecules, we can also understand the poorly explored chemical reactivity of the boron monoxide radicals. We will also compare the chemical reactivity of boron monoxide radicals with those of the isoelectronic cyano radical (CN; $X^2\Sigma^+$)[36] with allene.

2. EXPERIMENTAL SECTION

The gas phase reactions between boron monoxide radicals (BO; $X^2\Sigma^+$) and allene (H_2CCCH_2; X^1A_1) were carried out under single collision conditions in a universal crossed molecular beam machine.[42−46] A pulsed supersonic beam of ground state boron monoxide radicals were produced via laser ablation of boron rod[47] and simultaneous reaction of ablated boron atom with carbon dioxide (CO_2, 99.99%, BOC gases) carrier gas. Here, 266 nm (fourth-harmonic output of Spectra-Physics Quanta-Ray Pro 270 Nd:YAG laser) laser pulse operating at a repetition rate of 30 Hz was focused on a rotating boron rod with an output energy of 15−20 mJ/pulse. A pulsed carbon dioxide molecular beam was expanded in the ablation region from a pressure of 4 atm by a porch trickle pulsed valve[48] operating at a repetition rate of 60 Hz. Here, the supersonic beam of boron monoxide radical was produced most likely via the abstraction of an oxygen atom from carbon dioxide reactant and passed through a skimmer of diameter 1 mm followed by a four-slot chopper wheel to reach the interaction region. The chopper wheel selected 11.2 μs segment of the boron monoxide radical beam with a peak velocity (v_p) = 1421 ± 40 ms^{-1} and speed ratio (S) of 2.3 ± 0.3. A second porch trickle pulsed valve operating at a repetition rate of 60 Hz was used to supersonically expand allene (H_2CCCH_2; Aldrich, >99%) molecule from a pressure of 550 Torr in the secondary chamber. This secondary molecular beam of allene intersects the selected segment of the primary beam of ^{11}BO radicals perpendicularly in the interaction region. The segment of the secondary molecular beam intersecting with the primary beam was characterized by a peak velocity of 840 ± 10 ms^{-1} and speed ratio (S) of 12.0 ± 0.2. The collision energy between boron monoxide and allene was determined to be 22.0 ± 1.3 kJ mol^{-1}. In addition, we have also characterized the ro-vibrational states of $^{11}BO(X^2\Sigma^+)$ radicals by recording laser-induced fluorescence (LIF) spectra by probing the $A^2\Pi-X^2\Sigma^+$ transitions.[49] The LIF spectra were recorded within 422−436 nm (Nd:YAG pumped Lambda Physik Scanmate dye laser) range with 10 μJ/pulse. By comparing the LIF spectra recorded experimentally with the best fitted simulated spectra obtained using the diatomic spectral simulation program developed by Tan,[50] we have determined a value of 250 K as the rotational temperature of ^{11}BO radicals. This indicates that the ^{11}BO radicals have a maximum of 2.0 ± 0.3 kJ mol^{-1} of internal energy, and the experiments suggested that the population of the vibrationally excited ν = 1 level state is less than 5%.[49]

A rotatable triply differentially pumped quadrupole mass spectrometer (QMS) operating in the time-of-flight (TOF) mode was exploited to monitor the reactively scattered products following ionization via electron-impact ionization of about 80 eV electron energy.[42−46] The TOF spectra of the reactively scattered products were collected at an interval of 2.5° over the entire angular distribution. The recorded TOF spectra were integrated and normalized to extract the product angular distribution in the laboratory frame. A forward-convolution routine was employed to transform the experimental recorded data from laboratory frame into the center-of-mass reference frame.[51,52] This iterative method assumes an initial choice of angular flux distribution, $T(\theta)$, and the product translational energy distribution, $P(E_T)$, in the center-of-mass frame. The best fits were obtained by iteratively refining the adjustable parameters in the center-of-mass functions. The product flux contour map, $I(\theta,u) = P(u) \times T(\theta)$, reports the intensity of the reactively scattered products (I) as a function of the CM scattering angle (θ) and product velocity (u). This plot is called the reactive differential cross section and gives an image of the reaction.

3. THEORETICAL SECTION

We have also investigated the reaction of $^{11}BO(X^2\Sigma^+)$ and allene (X^1A_1) computationally. Here the geometries of stationary points, reactants, products intermediates, and transition states were optimized at the CCSD(T)-fc[53−56] level of theory using the cc-pVTZ[57,58] basis set. The vibrational frequencies and the zero point energies of the structures were computed at the CCSD(T)-fc/cc-pVTZ level of theory. The energies were further refined using a composite method described elsewhere.[27] The energies of $^{11}BOC_3H_4$ intermediates computed using the composite method are associated with an uncertainty ±9 kJ mol^{-1}. Here, ACES II[59] and NWChem 6.1[60,61] were used for the ab initio calculations. In addition to $^{11}BOC_3H_4$ PES, we have also calculated the rate constants of each reaction pathway and the branching ratios of the products utilizing RRKM theory.[62,63] For a reaction $A^* \xrightarrow{k} A^{\ddagger} \rightarrow P$, where A^*, $A^{\ddagger}$, and P represent energized reactant, the transition state, and the product, respectively, the rate constant $k(E)$ can be expressed as

$$k(E) = \frac{\sigma}{h}\frac{W^{\ddagger}(E - E^{\ddagger})}{\rho(E)}$$

where σ is the symmetry factor, $W^{\ddagger}$ the number of states of the transition state, $E^{\ddagger}$ the transition state energy, and ρ the density of states of the reactant. ρ and $W^{\ddagger}$ are computed by the saddle-point method, and molecules are treated as collections of harmonic oscillators whose harmonic frequencies are obtained by the composite method as mentioned above.[64]

4. RESULTS

4.1. Experimental Results. Reactive scattering signal for the reaction of boron monoxide $^{11}BO(X^2\Sigma^+)$ (27 amu) with allene (H_2CCCH_2, X^1A_1) (40 amu) was recorded at mass-to-charge ratios (m/z) of 66 ($^{11}BOC_3H_3^+$) and m/z = 65 ($^{11}BOC_3H_2^+/^{10}BOC_3H_3^+$) at a collision energy of 22.0 ± 1.3 kJ mol^{-1} for the atomic hydrogen and/or molecular hydrogen loss pathways, respectively. The TOF spectra at m/z = 66 ($^{11}BOC_3H_3^+$) clearly demonstrate that a molecular species of formula $^{11}BOC_3H_3$ were formed via a ^{11}BO radical versus atomic hydrogen exchange pathway. After scaling, the TOF spectra recorded at m/z = 66 and m/z = 65 were found to be identical, indicating that the ion signal at m/z = 65 originated from the dissociative ionization of the parent molecule $^{11}BOC_3H_3$ (66 amu) in the electron impact ionizer of the detector. Hence, we can conclude that the $^{11}BOC_3H_3$ product was formed in the reaction of ^{11}BO ($X^2\Sigma^+$) with allene (CH_2CCH_2, X^1A_1) via the boron monoxide versus atomic hydrogen loss pathway; further, the molecular hydrogen loss channel is found to be closed. The TOF spectra for the hydrogen atom loss channels are shown in Figure 2. We also attempted to monitor ions at m/z = 52 ($C_2H^{11}BO^+$) and m/z = 51 ($C_2{}^{11}BO^+/C_2H^{10}BO^+$) for the methyl loss channel as observed in the reaction of the boron monoxide radical with methylacetylene (CH_3CCH)[27] but did not observe any reactive scattering signal. This indicates that in the reaction of allene (CH_2CCH_2; 40 amu) plus boron monoxide (^{11}BO; 27 amu) no

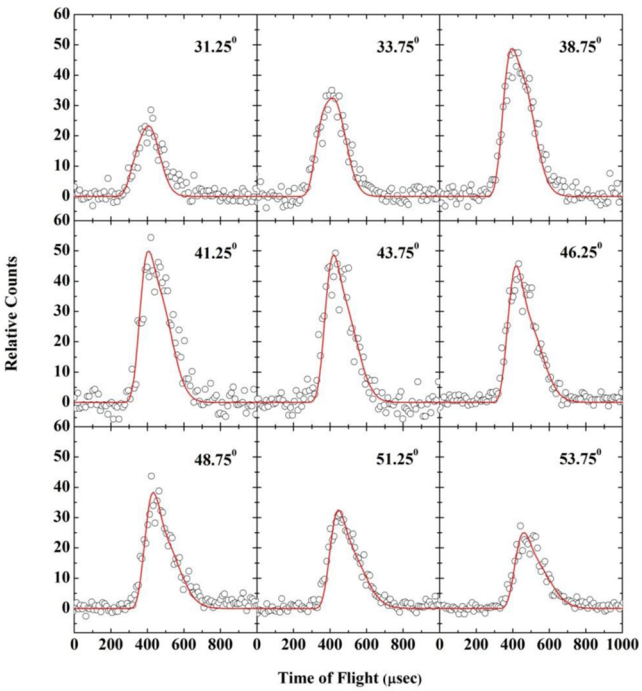

Figure 2. Time-of-flight data at various angles for the reaction between boron monoxide (^{11}BO; $X^2\Sigma^+$) with allene (CH_2CCH_2; X^1A_1) recorded at m/z = 66 at a collision energy of 22.0 ± 1.3 kJ mol^{-1}. The circles indicate the experimental data, and the solid lines indicate the calculated fit.

methyl loss channel is open. For the atomic hydrogen loss channel, the TOF spectra were recorded at various laboratory angles in 2.5° intervals. The laboratory angular distribution as shown in Figure 3 for the $^{11}BOC_3H_3$ product at m/z = 66 was obtained by integrating these TOF spectra recorded at various angles and the distribution extends at least 45° in the scattering plane as defined by the primary and the secondary beams. It should be mentioned that the primary motivations of recording time-of-flight (TOF) spectra are to measure the time taken by

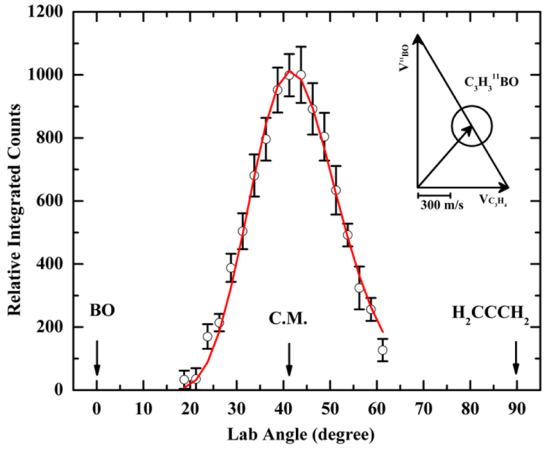

Figure 3. Laboratory angular distribution (LAB) of the $^{11}BOC_3H_3$ isomer(s) (m/z = 66) for the reaction of boron monoxide (^{11}BO; $X^2\Sigma^+$) with allene (CH_2CCH_2; X^1A_1) at collision energy of 22.0 ± 1.3 kJ mol^{-1}. The circles and error bars indicate the experimental data, and the solid line indicates the calculated distribution. The inset shows the Newton diagram of the reaction at a collision energy of 22.0 ± 1.3 kJ mol^{-1}.

the product to reach the detector. The laboratory angular distribution peaks at 41.2 ± 0.5° close to the center-of-mass (CM) angle of 41.3 ± 1.0°. The above observations along with the nearly symmetric laboratory angular distribution suggest that the reaction proceeds through indirect (complex forming) scattering dynamics involving the $^{11}BOC_3H_4$ reaction intermediate(s).[65] Note that the TOF spectra and the laboratory angular distribution can be fit using a *single channel* with a product combination of 66 amu ($^{11}BOC_3H_3$) and 1 amu (H) utilizing the center-of-mass functions as depicted in Figure 4.

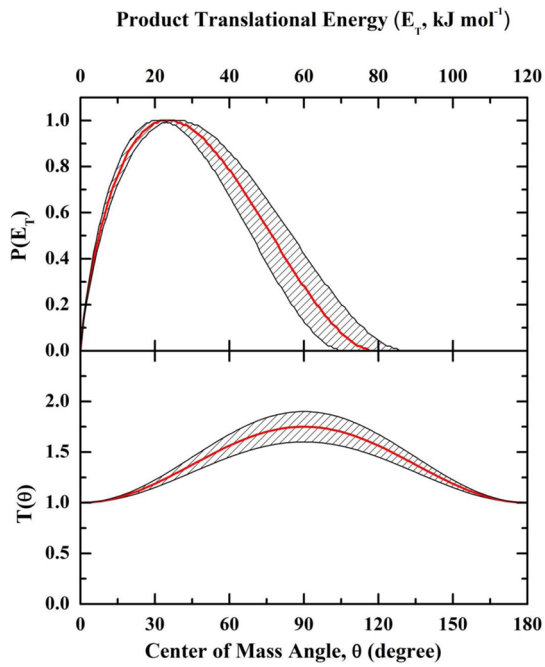

Figure 4. Center-of-mass translational energy distribution (top) and center-of-mass angular distribution (bottom) for the hydrogen loss pathway of the reaction between boron monoxide (^{11}BO; $X^2\Sigma^+$) with allene (CH_2CCH_2; X^1A_1). The hatched areas indicate the acceptable lower and upper limits of the fits, and the solid red line defines the best fit functions.

The analysis of the center-of-mass translational energy ($P(E_T)$) and center-of-mass angular distribution ($T(\theta)$) reveals crucial information on the chemical dynamics of the boron monoxide−allene system. Figure 4 (top) presents the center-of-mass translational energy distribution, $P(E_T)$, for the $^{11}BOC_3H_3$ plus atomic hydrogen channel. This distribution depicts a maximum translational energy release, E_{max}, of 77 ± 10 kJ mol^{-1}. For products formed without internal excitation, the maximum translational energy release presents the sum of the collision energy and the reaction exoergicity. Therefore, the exoergicity of the hydrogen loss channel can be extracted by subtracting the collision energy (22.0 ± 1.3 kJ mol^{-1}) from the maximum translational energy (77 ± 10 kJ mol^{-1}). This leads to a reaction exoergicity of 55 ± 11 kJ mol^{-1} to form $^{11}BOC_3H_3$ isomer(s) plus atomic hydrogen. It is worth mentioning that laser-induced florescence (LIF) study shows that ^{11}BO has been efficiently cooled by the supersonic expansion and only has a maximum of 2.0 ± 0.3 kJ mol^{-1} of internal energy. If the measured internal energy of the ^{11}BO radical (2.0 ± 0.3 kJ mol^{-1}) is distributed only into the translational degrees of freedom, it could be subtracted from the reaction exoergicity (55 ± 11 kJ mol^{-1}) to get a value of the reaction exoergicity of

53 ± 11 kJ mol^{-1}, assuming that allene is also efficiently cooled due to the supersonic expansion. Further, the maximum of the translational energy flux distribution is displaced from zero translational energy at about 18−28 kJ mol^{-1}. This finding suggests that at least one of the reaction channels to form the product $^{11}BOC_3H_3$ isomer(s) has an exit barrier and hence a tight exit transition state when the $^{11}BOC_3H_4$ intermediate decomposes to the product(s).[66] This tight exit transition state (repulsive bond rupture) involves a significant electron rearrangement. Finally, the center-of-mass translational energy distribution allows us to determine the average amount of energy released into the translational degrees of freedom of the products, i.e., 39 ± 7% of the total available energy.

The center-of-mass angular distribution, $T(\theta)$, delivers additional information on the chemical dynamics of the title reaction and is shown in Figure 4 (bottom). The distribution shows intensity over the whole angular range from 0° to 180°; this finding is indicative of indirect scattering dynamics involving the formation of $^{11}BOC_3H_4$ collision complex(es).[65] Second, the angular distribution is forward−backward symmetric with respect to 90°. This forward−backward symmetry implies that the lifetime of the decomposing $^{11}BOC_3H_4$ complexes, which emit the hydrogen atom, is longer than their rotation periods.[65] The best fit $T(\theta)$ depicts a distribution maximum at 90° which indicates a geometrical constraint in the exit channel.[65] Here, the distribution suggests that the hydrogen atom is emitted almost perpendicularly to the plane of the decomposing $^{11}BOC_3H_4$ complex, i.e., nearly parallel to the total angular momentum vector.[65] These findings are also compiled in the flux contour map (Figure 5). The flux contour map (Figure 5) gives an image of the reaction which shows an isotropic distribution and a sideway scattering pattern peaking at 90° as observed in Figure 4.

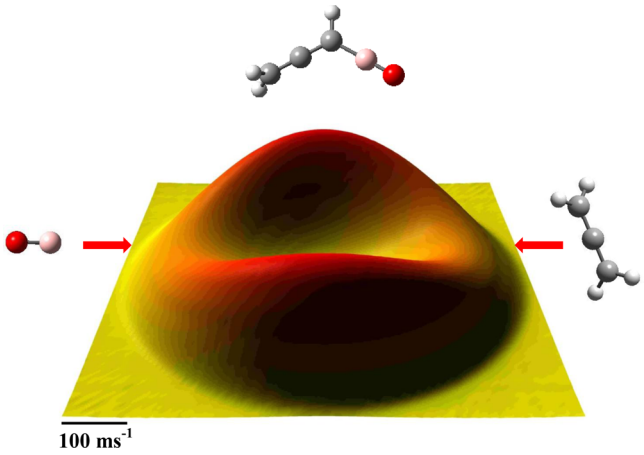

Figure 5. Flux contour maps of the atomic hydrogen loss pathway in the crossed molecular beam reaction of boron monoxide radical with allene leading to the formation of boronylallene ($CH_2CCH^{11}BO$).

4.2. Theoretical Results. The optimized structures of the reactants, products, intermediates, and transition states are compiled in Figures 6 and 7. The computations predict the existence of ten $^{11}BOC_3H_4$ reaction intermediates (**i1**−**i10**) and six potential product channels (**p1**−**p6**) involving atomic hydrogen loss (**p1**−**p3**), hydrogen abstraction (**p4**), carbon−carbon bond rupture (**p5**), and methyl radical elimination (**p6**). In detail, the reaction is suggested to proceed via the barrierless formation of a weakly bound van der Waals complex **i1** ($^{11}BOC_3H_4$), which is stabilized by 9 kJ mol^{-1} compared to the separated reactants. The molecular structure of **i1** (Figure 7) is characterized by a weak interaction between the boron atom of the boron monoxide radical and the π-electron density of the allene molecule. This van der Waals complex **i1** can undergo isomerization via an addition of ^{11}BO with its radical center to the C1 and/or the C2 carbon atom of the allene molecule forming intermediate **i2** (−175 kJ mol^{-1}) and/or **i3** (−264 kJ mol^{-1}), respectively. The inherent barriers to isomerization are 2 and 4 kJ mol^{-1}, respectively, and hence *below* the energy of the separated reactants indicating the presence of two submerged barriers in the entrance channel. Note that **i2** and **i3** are connected via a transition state located 67 kJ mol^{-1} above **i2**. Intermediate **i2** can undergo two competing unimolecular decomposition pathways via atomic hydrogen loss from the C3 and C1 carbon atoms of the allene moiety to form 3-propynyloxoborane ($CH_2(^{11}BO)CCH$; **p1**) and propadienyloxoborane (boronylallene) ($CH_2CCH^{11}BO$; **p2**), respectively. Both reactions proceed via tight exit transition states residing 19 and 24 kJ mol^{-1} above the separated products; the overall reactions are exoergic by 29 ± 9 and 46 ± 9 kJ mol^{-1}, respectively. Intermediate **i2** can also isomerizes to intermediates **i4** (−163 kJ mol^{-1}) and **i5** (−281 kJ mol^{-1}) via hydrogen atom migration. However, the calculated energy barrier of the **i2** → **i4** pathway is very high (198 kJ mol^{-1}) with the corresponding transition state residing 23 kJ mol^{-1} above the reactants. Considering the collision energy (22.0 ± 1.3 kJ mol^{-1}) and the competing decomposition of **i2** to **p1** and/or **p2**, the pathway **i2** → **i4** is expected to be energetically unfavorable. However, **i5**, formed by overcoming an energy barrier of 162 kJ mol^{-1}, can isomerize to **i4** via a BO migration (**i6**) followed by rapid cis/trans isomerization. From intermediates **i4** to **i6**, two atomic hydrogen loss pathways can lead to the products **p1** and **p2** by overcoming tight transition states located 28 and 24 kJ mol^{-1} above the separated products, respectively. The formation of acetylene (C_2H_2) and the methyleneoxoborane ($CH_2{}^{11}BO$) radical (**p5**) from intermediate **i4** is energetically unlikely considering the energetically favorable isomerization of **i4** to **i6**.

Now we shall discuss the fate of intermediate **i3**. Because of the resonance stabilization of the allyl moiety, **i3** is 89 kJ mol^{-1} more stable than **i2**. Note that **i3** cannot be associated with any decomposition pathway; instead, **i3** can isomerize to **i7** through a [1,3] atomic hydrogen migration via an energy barrier of 253 kJ mol^{-1}. Considering the molecular structure of **i7**, it is interesting to note that this intermediate can be also accessed via the reaction of the boron monoxide radical adding to the C2 position of the methylacetylene molecule.[27] Therefore, intermediate **i7** links the boron monoxide−allene and boron monoxide−methylacetylene systems. Intermediate **i7** can rapidly isomerize to **i8**. The latter can undergo a BO migration from the C2 to the C1 carbon atom yielding **i9**, which in turn can isomerize via cis−trans conversion to **i10**. Three products can be reached from **i8** to **i10**. First, an atomic hydrogen elimination from the methyl group of **i9**/**i10** can lead to propadienyloxoborane ($CH_2CCH^{11}BO$; **p2**) via exit transition states located 15 kJ mol^{-1} above the separated products. Second, **i9** can undergo an atomic hydrogen elimination from its central carbon atom to form 1-propynyloxoborane (**p3**) ($CH_3CC^{11}BO$; −74 ± 9 kJ mol^{-1}) via an exit transition barrier located 21 kJ mol^{-1} above the separated products. Finally, ethynyloxoborane (**p6**) ($HCC^{11}BO$; −86 ± 9 kJ mol^{-1}) can be formed via methyl loss from **i8** via a tight exit transition state

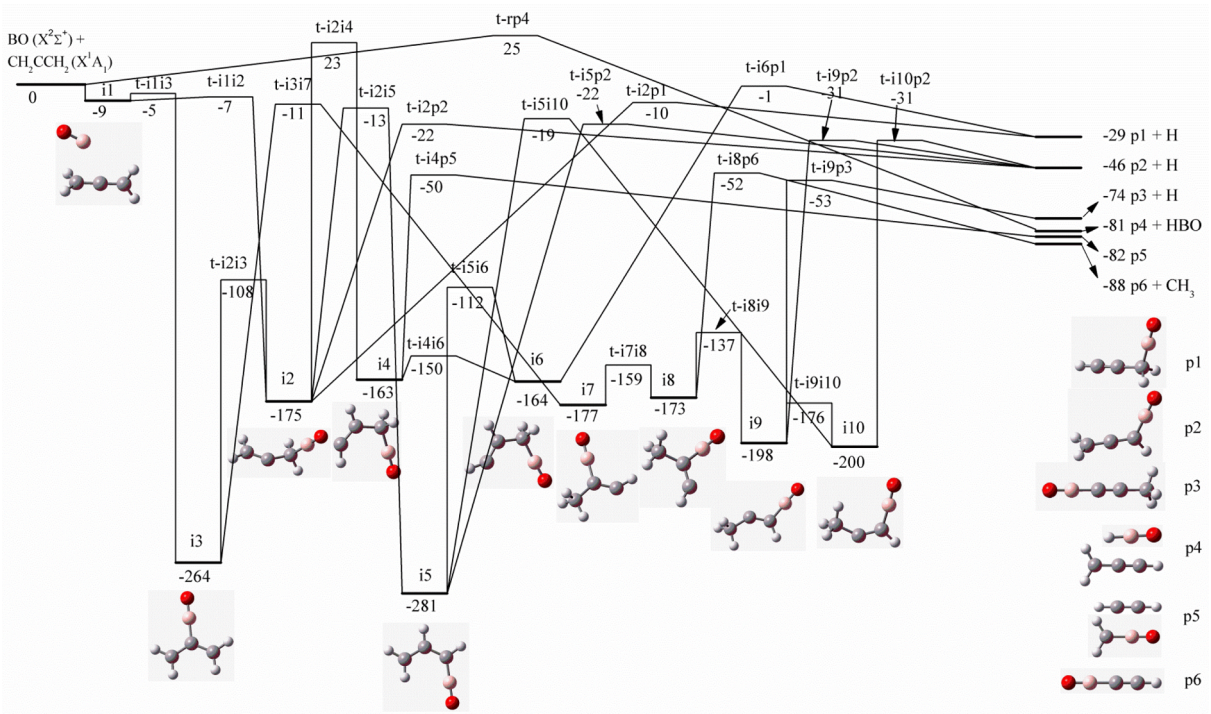

Figure 6. Schematic representation of the $^{11}BOC_3H_4$ potential energy surface.

located 36 kJ mol^{-1} above the separated products. Finally, we also investigated the direct hydrogen abstraction pathway from allene forming the H^{11}BO molecule and the CH_2CCH radical (**p4**). The transition state for this pathway is higher in energy than the reactants by 25 kJ mol^{-1}. Based on the collision energy (22.0 ± 1.3 kJ mol^{-1}) and the barrierless formation of intermediates **i1**, the abstraction pathway should be energetically unfavorable.

5. DISCUSSION

In order to investigate the underlying reaction mechanisms of the boron monoxide radical with allene, we are merging now the experimental results with the computational data. First, let us compile the experimental results. The TOF spectra recorded at m/z = 66 are indicative of the formation of product(s) with general formula $^{11}BOC_3H_3$. This clearly indicates that the atomic hydrogen loss pathway is open. Any methyl loss channel was found to be closed or below our detection limit. The center-of-mass angular distribution ($T(\theta)$) clearly depicts that the reaction followed indirect scattering dynamics via long-lived $^{11}BOC_3H_4$ collision complex(es). Further the $T(\theta)$ distribution maximum at 90° suggests a preferential atomic hydrogen loss direction perpendicular to the rotational plane of the decomposing complex(es). The formation of $^{11}BOC_3H_3$ isomer(s) plus atomic hydrogen is found to be exoergic by 55 ± 11 kJ mol^{-1}, and at least one of the atomic hydrogen loss pathways involve a tight exit transition barrier in the order of 18−28 kJ mol^{-1}. Since, under single collision conditions, only the hydrogen atom loss pathway(s) is (are) open, we are comparing first the experimentally derived reaction energy with the computed values to form product isomers with the general formula $^{11}BOC_3H_3$. Based on electronic structure calculations, three distinct $^{11}BOC_3H_3$ isomers, 3-propynyloxoborane ($CH_2(^{11}BO)$ CCH; **p1**), propadienyloxoborane ($CH_2CCH^{11}BO$; **p2**), and 1-propynyloxoborane (CH_3CC^{11}BO; **p3**), can be formed with overall reaction exoergicities of 29 ± 9, 46 ± 9, and 74 ± 9 kJ mol^{-1}, respectively. The crossed molecular beam data verify a reaction exoergicity of 55 ± 11 kJ mol^{-1}; this data correlates nicely with the computed reaction exoergicity of 46 ± 9 kJ mol^{-1} to form propadienyloxoborane ($CH_2CCH^{11}BO$; **p2**) plus atomic hydrogen. Hence, **p2** is the most likely major reaction product. However, we cannot exclude additional contributions of the thermodynamically less favorable product **p1** based on these data alone. Therefore, we investigated the sensitivity of our single channel fits via an artificial incorporation of an additional pathway leading to the formation of a $^{11}BOC_3H_3$ isomer and a hydrogen atom. Here, we find that a contribution of an additional reaction channel (10−15%) with a reaction exoergicity of 29 ± 9 kJ mol^{-1} associated with the formation of 3-propynyloxoborane ($CH_2(^{11}BO)CCH$; **p1**) does not change our fits notably. Therefore, on the basis of these observations, we propose that **p2** (CH_2CCH^{11} BO) is the dominant reaction product with *possible* minor contributions from **p1** ($CH_2(^{11}BO)$ CCH).

We are now proposing the underlying reaction mechanisms by combining the experimental data with the electronic structure and statistical calculations. A comparison of the molecular structures of the reactants with those of the products **p2** (major) and **p1** (minor) suggests the replacement of a hydrogen atom in the allene reactant by the boron monoxide radical. Here, the reaction proceeds via indirect scattering dynamics via the formation of a van der Waals complex **i1**, which isomerizes preferentially via addition of the boron monoxide radical with its radical center at the boron atom through a submerged barrier to form **i2**. The latter decomposes via atomic hydrogen loss from the C1 carbon atom forming propadienyloxoborane ($CH_2CCH^{11}BO$; **p2**) (major) and 3-propynyloxoborane ($CH_2(^{11}BO)CCH$; **p1**) (minor) involving tight exit transition states. Specifically, the computations suggest a tight exit transition state located 24 kJ mol^{-1} above the energy of the separated products. This data correlates very

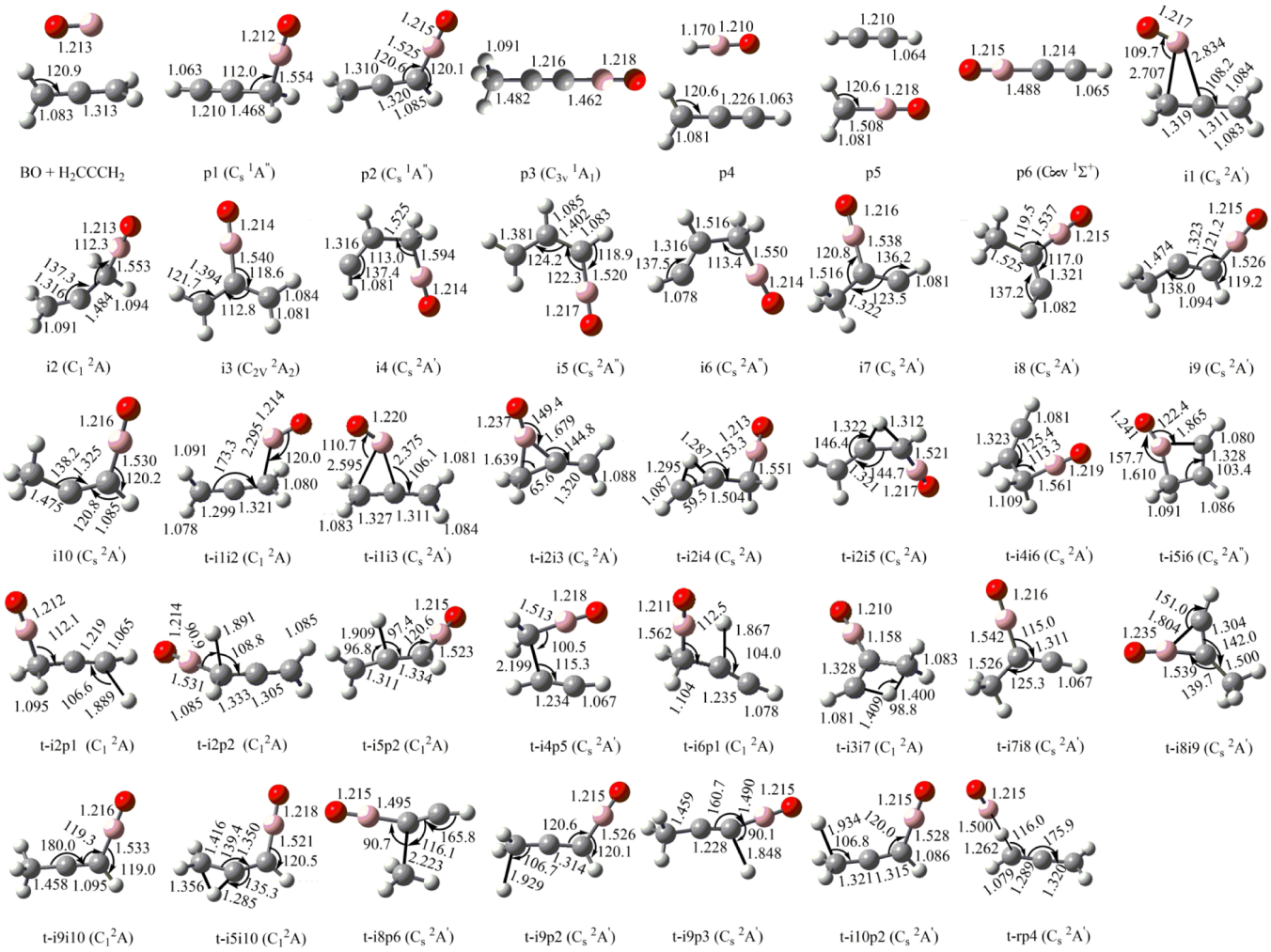

Figure 7. Structures of relevant stationary points (products, intermediates, and transition states) on the $^{11}BOC_3H_4$ potential energy surface (PES). Angles and bond lengths are shown in degrees and angstroms, respectively.

well with the experimental finding that a tight exit transition state resides about 18−28 kJ mol^{-1} above the separated products. The existence of an exit barrier from intermediate **i2** to **p2** (24 kJ mol^{-1}) is sensible as the reversed reaction; i.e., the hydrogen atom addition to a closed shell substituted allene molecule would have an associated entrance barrier. Further, the calculated geometry of the exit transition state from **i2** to **p2** (Figure 7) suggests a direction of the atomic hydrogen emission almost perpendicularly (90.9°) to the molecular plane. This geometry is predicted based on the detailed shape of the center-of-mass angular distribution of the atomic hydrogen loss pathway.

Can these findings also explain why the thermodynamically most stable 1-propynyloxoborane isomer (**p3**) ($CH_3CC^{11}BO$) is not being formed? Note that the formation of **p3** would require the unimolecular decomposition of **i9**, which in turn is accessed via migration of the boron monoxide moiety involving intermediate **i8**. Recall that both **i8** and **i9** have been shown to present central reaction intermediates in the reaction of the boron monoxide radical with methylacetylene involving three competing reaction mechanisms via two distinct atomic hydrogen losses and a methyl group elimination leading to 1-propynyloxoborane ($CH_3CC^{11}BO$) (**p3**) and propadienyloxoborane ($CH_2CCH^{11}BO$) (**p2**) via atomic hydrogen loss as well as ethynyloxoborane ($HCC^{11}BO$) (**p6**) plus a methyl group.[27] The branching ratios of these channels forming $CH_2CCH^{11}BO$, $CH_3CC^{11}BO$, and $HCC^{11}BO$ were derived to be 4 ± 3%, 40 ± 5%, and 56 ± 15%, respectively. Therefore, the existence of intermediates **i7** to **i10** in the reaction of the boron monoxide radical with allene *must* be reflected in the detection of the methyl loss pathway leading to **p6**. Since the methyl loss channel was not observed in the reaction of the boron monoxide radical with allene, but only in the boron monoxide−methyl acetylene system, we can conclude that intermediates **i7** to **i10** cannot be accessed in the boron monoxide−allene system. The potential energy surface indicates that **i7** can be only accessed via intermediate **i3** through hydrogen migration involving a barrier of 253 kJ mol^{-1}. This barrier is considerably higher than the barrier involved in the isomerization of **i3** to **i2** (156 kJ mol^{-1}), thus making the **i3** → **i7** pathway less likely than the **i3** → **i2** isomerization. Therefore, we can conclude that **i7** cannot be accessed in the reaction of the boron monoxide radical with allene. As a consequence, the reaction sequences **i7** → **i8** → **i9** → **p3** and **i7** → **i8** → **p6** are also closed, and the thermodynamically most stable isomer **p3** cannot be formed in the reaction of the boron monoxide radical with allene. Our statistical RRKM calculations at 22.0 kJ mol^{-1} fully support our conclusions suggesting that boronylallene ($H_2CCCH^{11}BO$) presents the major product (98.3%) with 3-propynyloxoborane

($CH_2(^{11}BO)CCH$) and 1-propynyloxoborane ($CH_3CC^{11}BO$) having fractions of only 1.5% and 0.2%, respectively. The statistical (RRKM) calculations were performed considering 100% initial population of the intermediate **i1** (van der Waals complex).

The boron monoxide radical also represents an interesting system from the physical organic chemistry viewpoint due to its isoelectronic character with the cyano radical (CN; $X^2\Sigma^+$). Here we compare the title reaction with the reaction of the cyano radical (CN; $X^2\Sigma^+$) and allene studied previously by our group experimentally and theoretically.[36] Both the reactions proceed via de facto barrierless additions of the radical to the C1 and/or C2 carbon atom of allene reactant forming reaction intermediates CH_2CCH_2X and $CH_2C(X)CH_2$ (X = BO, CN), respectively, via indirect scattering dynamics. These doublet radical intermediates are stabilized by 175−264 kJ mol^{-1} (X = BO) and 219−321 kJ mol^{-1} (X = CN), respectively; these energetics indicate the formation of a stronger carbon−carbon (X = CN) bond compared to weaker carbon−boron (X = BO) bond (typically by 50 kJ mol^{-1}). In both cases, the reaction proceeds mostly via the addition of X (BO, CN) with its electrophilic center (B in BO and C in CN) to the terminal carbon atom (C1) of the allene forming $CH_2CCH_2{}^{11}X$ (X = BO, CN) intermediate. The resultant intermediate $CH_2CCH_2{}^{11}X$ undergoes unimolecular decomposition predominantly via the atomic hydrogen elimination from the terminal CH_2X group which leads to the formation substituted allene CH_2CCHX (X = BO, CN) product. The decomposition pathways to the products CH_2CCHX (X = BO, CN) involve tight exit transition states located 24 kJ mol^{-1} (X = BO) and 18 kJ mol^{-1} (X = CN), respectively, above the separated products; finally, the products are formed via overall exoergic reactions (X = BO: −46 kJ mol^{-1}; X = CN: −86 kJ mol^{-1}). The enhanced reaction exoergicity of the cyano−allene system can be once again related to the enhanced C−C bond strength compared to the C−B bond in the BO−allene system. A minor product channel is also observed in both the systems leading to the formation of substituted methylacetylene products $CH_2(X)$-CCH (X = BO, CN) via atomic hydrogen elimination from the terminal CH_2 group of the intermediate CH_2CCH_2X (X = BO, CN). Based on the statistical analysis, the products CH_2CCHX versus $CH_2(X)CCH$ (X = BO, CN) ratios are 66:1 (X = BO) and 9:1 (X = CN).

6. CONCLUSION

We have investigated the gas phase reaction of boron monoxide radical (^{11}BO; $X^2\Sigma^+$) with allene (CH_2CCH_2; X^1A_1) at a collision energy of 22.0 ± 1.3 kJ mol^{-1}. Combined with computed data, the experimental results suggest that the reaction dynamics were indirect and the reaction proceeded via the formation of a $^{11}BOC_3H_4$ van der Waals complex. The resulting intermediate $^{11}BOC_3H_4$ undergoes isomerization predominantly via the addition of boron monoxide with its boron atom to the terminal carbon atom (C1) of the allene forming $CH_2CCH_2{}^{11}BO$ intermediate. The latter can undergo unimolecular decomposition via atomic hydrogen elimination from the terminal carbon atom holding the boronyl group through a tight exit transition state to synthesize the boronylallene product ($H_2CCCH^{11}BO$) in a slightly exoergic reaction (55 ± 11 kJ mol^{-1}). Two additional minor atomic hydrogen loss channels have also been suggested based on the statistical RRKM calculation leading to the formation of the products 3-propynyloxoborane ($CH_2(^{11}BO)CCH$) and 1-propynyloxoborane ($CH_3CC^{11}BO$) with fractions of 1.5% and 0.2%, respectively. A comparison of the reaction of allene with the boron monoxide radical and its isoelectronic cyano radical revealed that both the reactions proceed via the addition through their radical center (B in BO; C in CN) to the terminal carbon atom of the allene molecule followed by an atomic hydrogen elimination yielding mainly substituted allene product CH_2CCHX (X = BO, CN). The present gas phase synthesis and characterization of organyloxoboranes (RBO) can further be utilized as a tool to investigate the chemistry of reactive oxoborane intermediates.

■ ASSOCIATED CONTENT

Supporting Information

Relative energies with respect to reactants in kJ mol^{-1} and Cartesian coordinates (Å) of reactants, intermediates, products, and transition states optimized at the CCSD(T)-fc/cc-pVTZ level of theory; rate constant of each reaction pathway and branching ratios of the products calculated using statistical RRKM theory at the collision energy of 22.0 kJ mol^{-1}. This material is available free of charge via the Internet at http://pubs.acs.org.

■ AUTHOR INFORMATION

Corresponding Authors

*E-mail ralfk@hawaii.edu (R.I.K.).
*E-mail bartlett@qtp.ufl.edu (R.J.B.).

Notes

The authors declare no competing financial interest.

■ ACKNOWLEDGMENTS

This work was supported by the Air Force Office of Scientific Research by grant FA9550-12-1-0213 to the Kaiser group and by grant FA 9550-11-1-0065 to the Bartlett group.

■ REFERENCES

(1) Iwadate, N.; Suginome, M. Differentially Protected Diboron for Regioselective Diboration of Alkynes: Internal-Selective Cross-Coupling of 1-Alkene-1,2-diboronic Acid Derivatives. *J. Am. Chem. Soc.* **2010**, *132*, 2548−2549.

(2) Noguchi, H.; Hojo, K.; Suginome, M. Boron-Masking Strategy for the Selective Synthesis of Oligoarenes via Iterative Suzuki−Miyaura Coupling. *J. Am. Chem. Soc.* **2007**, *129*, 758−759.

(3) Iwadate, N.; Suginome, M. Synthesis of Masked Haloareneboronic Acids via Iridium-Catalyzed Aromatic C−H Borylation with 1,8-Naphthalenediaminatoborane (danBH). *J. Organomet. Chem.* **2009**, *694*, 1713−1717.

(4) Noguchi, H.; Shioda, T.; Chou, C.-M.; Suginome, M. Differentially Protected Benzenediboronic Acids: Divalent Cross-Coupling Modules for the Efficient Synthesis of Boron-Substituted Oligoarenes. *Org. Lett.* **2008**, *10*, 377−380.

(5) Gao, X.; Hall, D. G. 3-Boronoacrolein as an Exceptional Heterodiene in the Highly Enantio- and Diastereoselective Cr(III)-Catalyzed Three-Component [4 + 2]/Allylboration. *J. Am. Chem. Soc.* **2003**, *125*, 9308−9309.

(6) Crudden, C. M.; Hleba, Y. B.; Chen, A. C. Regio- and Enantiocontrol in the Room-Temperature Hydroboration of Vinyl Arenes with Pinacol Borane. *J. Am. Chem. Soc.* **2004**, *126*, 9200−9201.

(7) Ros, A.; Aggarwal, V. K. Complete Stereoretention in the Rhodium-Catalyzed 1,2-Addition of Chiral Secondary and Tertiary Alkyl Potassium Trifluoroborate Salts to Aldehydes. *Angew. Chem., Int. Ed.* **2009**, *48*, 6289−6292.

(8) Fournier, J.-H.; Maris, T.; Wuest, J. D.; Guo, W.; Galoppini, E. Molecular Tectonics. Use of the Hydrogen Bonding of Boronic Acids

To Direct Supramolecular Construction. *J. Am. Chem. Soc.* **2003**, *125*, 1002−1006.

(9) Maly, K. E.; Malek, N.; Fournier, J.-H.; Rodriguez-Cuamatzi, P.; Maris, T.; Wuest, J. D. Engineering Crystals Built from Molecules Containing Boron. *Pure Appl. Chem.* **2006**, *78*, 1305−1321.

(10) Rogowska, P.; Cyranski, M. K.; Sporzynski, A.; Ciesielski, A. Evidence for Strong Heterodimeric Interactions of Phenylboronic Acids with Amino Acids. *Tetrahedron Lett.* **2006**, *47*, 1389−1393.

(11) Hall, D. G. *Structure, Properties, and Preparation of Boronic Acis Derivatives*; Wiley-VCH: Weinheim, Germany, 2005.

(12) Fischer, R. C.; Power, P. P. π-Bonding and the Lone Pair Effect in Multiple Bonds Involving Heavier Main Group Elements: Developments in the New Millennium. *Chem. Rev.* **2010**, *110*, 3877−3923.

(13) Wang, Y.; Hu, H.; Zhang, J.; Cui, C. Comparison of Anionic and Lewis Acid Stabilized N-Heterocyclic Oxoboranes: Their Facile Synthesis from a Borinic Acid. *Angew. Chem., Int. Ed.* **2011**, *50*, 2816−2819.

(14) Kawashima, Y.; Endo, E.; Kawaguchi, K.; Hirota, E. Detection and Equilibrium Molecular Structure of a Short-Lived Molecule, HBO, by Microwave Spectroscopy. *Chem. Phys. Lett.* **1987**, *135*, 441−445.

(15) Lanzisera, D. V.; Andrews, L. Reactions of Laser-Ablated Boron Atoms with Methanol. Infrared Spectra and ab Initio Calculations of CH_3BO, CH_2BOH, and CH_2BO in Solid Argon. *J. Phys. Chem. A* **1997**, *101*, 1482−1487.

(16) Andrews, L.; Burkholder, T. R. Infrared Spectra of Boron Atom-Water Molecule Reaction Products Trapped in Solid Argon. *J. Phys. Chem.* **1991**, *95*, 8554−8560.

(17) Bettinger, H. F. Reversible Formation of Organyl(oxo)boranes (RBO) (R = C_6H_5 or CH_3) from Boroxins ($(RBO)_3$): A Matrix Isolation Study. *Organometallics* **2007**, *26*, 6263−6267.

(18) Pachaley, B.; West, R. Synthesis of a 1,3-dioxa-2,4-diboretane, an Oxoborane Precursor. *J. Am. Chem. Soc.* **1985**, *107*, 2987−2988.

(19) Bock, H.; Cederbaum, L.; Niessen, W. V.; Paezzold, P.; Rosmus, P.; Solouki, B. Methylboron Oxide, H_3C-B≡O. *Angew. Chem., Int. Ed.* **1989**, *28*, 88−90.

(20) Ito, M.; Tokitoh, N.; Okazaki, R. A Novel Approach to an Oxoborane and Its Lewis Base Complex. *Tetrahedron Lett.* **1997**, *38*, 4451−4454.

(21) Braunschweig, H.; Radacki, K.; Schneider, A. Oxoboryl Complexes: Boron-Oxygen Tripple Bonds Stabilized in the Coordication Sphere of Platinum. *Science* **2010**, *328*, 345−347.

(22) Braunschweig, H.; Radacki, K.; Schneider, A. Cyclodimerization of an Oxoboryl Complex Induced by Trans Ligand Abstraction. *Angew. Chem., Int. Ed.* **2010**, *49*, 5993−5996.

(23) Chang, Y.; Li, Q.-S.; Xie, Y.; King, R. B.; Schaefer, H. F., III Binuclear Iron Boronyl Carbonyls Isoelectronic with the Well-Known Decacarbonyldimanganese. *New J. Chem.* **2012**, *36*, 1022−1030.

(24) Chang, Y.; Li, Q.-S.; Xie, Y.; King, R. B. Prospects for Three-Electron Donor Boronyl (BO) Ligands and Dioxodiborene (B_2O_2) Ligands as Bridging Groups in Binuclear Iron Carbonyl Derivatives. *Inorg. Chem.* **2012**, *51*, 8904−8915.

(25) Parker, D. S. N.; Zhang, F.; Maksyutenko, P.; Kaiser, R. I.; Chang, A. H. H. A Crossed Beam and Ab Initio Investigation of The Reaction of Boron Monoxide (BO) with Acetylene (C_2H_2). *Phys. Chem. Chem. Phys.* **2011**, *13*, 8560−8570.

(26) Parker, D. S. N.; Zhang, F.; Maksyutenko, P.; Kaiser, R. I.; Chen, S. H.; Chang, A. H. H. A Crossed Beam and Ab Initio Investigation on the Formation of Vinyl Boron Monoxide (C_2H_3BO) via Reaction of Boron Monoxide (BO) with Ethylene (C_2H_4). *Phys. Chem. Chem. Phys.* **2012**, *14*, 11099−11106.

(27) Maity, S.; Parker, D. S. N.; Dangi, B. B.; Kaiser, R. I.; Fau, S.; Perera, A.; Bartlett, R. J. A Crossed Molecular Beam and Ab-Initio Investigation of the Reaction of Boron Monoxide (BO; $X^2\Sigma^+$) with Methylacetylene (CH_3CCH; X^1A_1) − Competing Atomic Hydrogen and Methyl Loss Pathways. *J. Phys. Chem. A* **2013**, *117*, 11794−11807.

(28) Parker, D. S. N.; Dangi, B. B.; Balucani, N.; Stranges, D.; Mebel, A. M.; Kaiser, R. I. Gas-Phase Synthesis of Phenyl Oxoborane (C_6H_5BO) via the Reaction of Boron Monoxide with Benzene. *J. Org. Chem.* **2013**, *78*, 11896−11900.

(29) Parker, D. S. N.; Balucani, N.; Stranges, D.; Kaiser, R. I.; Mebel, A. M. A Crossed Beam and ab Initio Investigation on the Formation of Boronyldiacetylene ($HCCCC^{11}BO$; $X^1\Sigma^+$) via the Reaction of the Boron Monoxide Radical (^{11}BO; $X^2\Sigma^+$) with Diacetylene (C_4H_2; $X^1\Sigma_g^+$). *J. Phys. Chem. A* **2013**, *117*, 8189−8198.

(30) Zhai, H.-J.; Li, S.-D.; Wang, L.-S. Boronyls as Key Structural Units in Boron Oxide Clusters: $B(BO)_2$- and $B(BO)_3$. *J. Am. Chem. Soc.* **2007**, *129*, 9254−9255.

(31) Li, S.-D.; Guo, J.-C.; Ren, G.-M. Density Functional Theory Investigations on Boronyl-Substituted Ethylenes $C_2H_{4-m}(BO)_m$ (m = 1−4) and Acetylenes $C_2H_{2-m}(BO)_m$ (m = 1, 2). *J. Mol. Struct.* **2007**, *821*, 153−159.

(32) Ollivier, C.; Renaud, P. Organoboranes as a Source of Radicals. *Chem. Rev.* **2001**, *101*, 3415−3434.

(33) Papakondylis, A.; Mavridis, A. Structure and Bonding of the Polytopic Molecule Li[BO]. A Theoretical Investigation. *J. Phys. Chem. A* **2001**, *105*, 7106−7110.

(34) Huang, L. C. L.; Asvany, O.; Chang, A. H. H.; Balucani, N.; Lin, S. H.; Lee, Y. T.; Kaiser, R. I.; Osamura, Y. Crossed Beam Reaction of Cyano Radicals with Hydrocarbon Molecules. IV. Chemical Dynamics of Cyanoacetylene (HCCCN; $X^1\Sigma^+$) Formation from Reaction of $CN(X^2\Sigma^+)$ with Acetylene, $C_2H_2(X^1\Sigma^+_g)$. *J. Chem. Phys.* **2000**, *113*, 8656−8666.

(35) Balucani, N.; Asvany, O.; Chang, A. H. H.; Lin, S. H.; Lee, Y. T.; Kaiser, R. I.; Osamura, Y. Crossed Beam Reaction of Cyano Radicals with Hydrocarbon Molecules. III. Chemical Dynamics of Vinyl Cyanide (C_2H_3CN;$X\ ^1A'$) Formation from Reaction of $CN(X^1\Sigma^+_g)$ with Ethylene, $C_2H_4(X\ ^1A_g)$. *J. Chem. Phys.* **2000**, *113*, 8643−8655.

(36) Balucani, N.; Asvany, O.; Kaiser, R. I.; Osamura, Y. Formation of Three C_4H_3N Isomers from the Reaction of $CN(X^2\Sigma^+)$ with Allene, H_2CCCH_2 (X^1A_1), and Methylacetylene, CH_3CCH (X^1A_1): A Combined Crossed Beam and Ab Initio Study. *J. Phys. Chem. A* **2002**, *106*, 4301−4311.

(37) Gu, X.; Zhang, F.; Kaiser, R. I. Reaction Dynamics on the Formation of 1- and 3-Cyanopropylene in the Crossed Beams Reaction of Ground State Cyano Radicals (CN) with Propylene (C_3H_6) and Its Deuterated Isotopologues. *J. Phys. Chem. A* **2008**, *112*, 9607−9613.

(38) Balucani, N.; Asvany, O.; Chang, A. H. H.; Lin, S. H.; Lee, Y. T.; Kaiser, R. I.; Bettinger, H. F.; Schleyer, P. V. R.; Schaefer, H. F., III. Crossed Beam Reaction of Cyano Radicals with Hydrocarbon Molecules. II. Chemical Dynamics of 1-Cyano-1-Methylallene ($CNCH_3CCCH_2$; X^1A') Formation from Reaction of $CN(X^2\Sigma^+)$ with Dimethylacetylene, CH_3CCCH_3 (X^1A_1'). *J. Chem. Phys.* **1999**, *111*, 7472−7479.

(39) Zhang, F.; Kim, S.; Kaiser, R. I.; Jamal, A.; Mebel, A. M. A Crossed Beams and Ab Initio Investigation on the Formation of Cyanodiacetylene in the Reaction of Cyano Radicals with Diacetylene. *J. Chem. Phys.* **2009**, *130*, 234308.

(40) Balucani, N. A. O.; Chang, A. H. H.; Lin, S. H.; Lee, Y. T.; Kaiser, R. I.; Bettinger, H. F.; Schleyer, P. V. R.; Schaefer, H. F., III Crossed Beam Reaction of Cyano Radicals with Hydrocarbon Molecules. I. Chemical Dynamics of Cyanobenzene (C_6H_5CN; X^1A_1) and Perdeutero Cyanobenzene (C_6D_5CN; X^1A_1) Formation from Reaction of $CN(X^2\Sigma^+)$ with Benzene, $C_6H_6(X^1A_{1g})$, and D6-Benzene, $C_6D_6(X^1A_{1g})$. *J. Chem. Phys.* **1999**, *113*, 7457−7471.

(41) Kaiser, R. I.; Balucani, N. The Formation of Nitriles in Hydrocarbon-Rich Atmospheres of Planets and Their Satellites: Laboratory Investigations by the Crossed Molecular Beam Technique. *Acc. Chem. Res.* **2001**, *34*, 699−706.

(42) Gu, X.; Guo, Y.; Zhang, F.; Mebel, A. M.; Kaiser, R. I. Reaction Dynamics of Carbon-Bearing Radicals in Circumstellar Envelopes of Carbon Stars. *Faraday Discuss.* **2006**, *133*, 245−275.

(43) Gu, X.; Guo, Y.; Kaiser, R. I. Mass Spectrum of the Butadiynyl Radical (C_4H; $X^2\ \Sigma^+$). *Int. J. Mass Spectrom.* **2005**, *246*, 29−34.

(44) Gu, X. B.; Guo, Y.; Kawamura, E.; Kaiser, R. I. Design of a Convection-Cooled, Cluster-Based Voltage Divider Chain for Photomultiplier Tubes. *Rev. Sci. Instrum.* **2005**, *76*, 083115.
(45) Guo, Y.; Gu, X.; Kaiser, R. I. Mass Spectrum of the 1-Butene-3-yne-2-yl Radical (i-C_4H_3; X^2A'). *Int. J. Mass Spectrom.* **2006**, *249/250*, 420−425.
(46) Guo, Y.; Gu, X.; Kawamura, E.; Kaiser, R. I. Design of a Modular and Versatile Interlock System for Ultrahigh Vacuum Machines: A Crossed Molecular Beam Setup as a Case Study. *Rev. Sci. Instrum.* **2006**, *77*, 034701.
(47) Gu, X.; Guo, Y.; Kawamura, E.; Kaiser, R. I. Characteristics and Diagnostics of an Ultrahigh Vacuum Compatible Laser Ablation Source for Crossed Molecular Beam Experiments. *J. Vac. Sci. Technol.* **2006**, *24*, 505−511.
(48) Proch, D.; Trickl, T. A High-Intensity Multi-Purpose Piezoelectric Pulsed Molecular Beam Source. *Rev. Sci. Instrum.* **1989**, *60*, 713−716.
(49) Maksyutenko, P.; Parker, D. S. N.; Zhang, F.; Kaiser, R. I. An LIF Characterization of Supersonic BO and CN Radical Sources for Crossed Beam Studies. *Rev. Sci. Instrum.* **2011**, *82*, 083107.
(50) Tan, X. CyberWit, 1.4.1.1 ed., 2004.
(51) Vernon, M. Ph.D Thesis, University of California, Berkley, 1981.
(52) Weis, M. S. Ph.D Thesis, University of California, Berkley, 1986.
(53) Raghavachari, K.; Trucks, G. W.; Pople, J. A.; Head-Gordon, M. A Fifth-Order Perturbation Comparison of Electron Correlation Theories. *Chem. Phys. Lett.* **1989**, *157*, 479−483.
(54) Bartlett, R. J.; Watts, J. D.; Kucharsky, S. A.; Noga, J. Non-Iterative Fifth-Order Triple and Quadruple Excitation Energy Corrections in Correlated Methods. *Chem. Phys. Lett.* **1990**, *165*, 513−522.
(55) Gauss, J.; Lauderdale, W. J.; Stanton, J. F.; Watts, J. D.; Bartlett, R. J. Analytic Energy Gradients for Open-Shell Coupled-Cluster Singles and Doubles (CCSD) Calculations Using Restricted Open-Shell Hartree-Fock (ROHF) Reference Functions. *Chem. Phys. Lett.* **1991**, *182*, 207−215.
(56) Watts, J. D.; Gauss, J.; Bartlett, R. J. Coupled-Cluster Methods with Noniterative Triple Excitations for Restricted Open-Shell Hartree-Fock and Other General Single Determinant Reference Functions. *J. Chem. Phys.* **1993**, *98*, 8718−8733.
(57) Dunning, T. H., Jr. Gaussian Basis Sets for Use in Correlated Molecular Calculations. I. The Atoms Boron through Neon and Hydrogen. *J. Chem. Phys.* **1989**, *90*, 1007−1023.
(58) Woon, D. E.; Dunning, T. H., Jr. Gaussian Basis Sets for Use in Correlated Molecular Calculations. V. Core-Valence Basis Sets for Boron through Neon. *J. Chem. Phys.* **1995**, *103*, 4572−4585.
(59) ACES-II is a program product of the Quantum Theory Project , University of Florida. Authors: Stanton, J. F.; Gauss, J.; Perera, S. A.; Watts, J. D.; Yau, A. D.; Nooijen, M.; Oliphant, N.; Szalay, P. G.; Lauderdale, W. J.; Gwaltney, S. R. et al. Integral packages included are VMOL (Almlöf, J.; Taylor, P. R.); VPROPS (Taylor, P.); ABACUS (Helgaker, T.; Jensen, H. J. Aa.; Jørgensen, P.; Olsen, J.; Taylor, P. R.); HONDO/GAMESS (Schmidt, M. W.; Baldridge, K. K.; Boatz, J. A.; Elbert, S. T.; Gordon, M. S.; Jensen, J. J.; Koseki, S.; Matsunaga, N.; Nguyen, K. A. ; Su, S.; Windus, T. L.; Dupuis, M.; Montgomery, J. A.).
(60) Valiev, M.; Bylaska, E. J.; Govind, N.; Kowalski, K.; Straatsma, T. P.; van Dam, H. J. J.; Wang, D.; Nieplocha, J.; Apra, E.; Windus, T. L.; de Jong, W. A. NWChem: A Comprehensive and Scalable Open-Source Solution for Large Scale Molecular Simulations. *Comput. Phys. Commun.* **2010**, *181*, 1477−1489.
(61) Hirata, S. Tensor Contraction Engine: Abstraction and Automated Parallel Implementation of Configuration-Interaction, Coupled-Cluster, and Many-Body Perturbation Theories. *J. Phys. Chem. A* **2003**, *107*, 9887−9897.
(62) Levine, R. D. *Molecular Reaction Dynamics*; Cambridge University Press: Cambridge, 2005.
(63) Nguyen, T. L.; Mebel, A. M.; Lin, S. H.; Kaiser, R. I. Product Branching Ratios of the $C(^3P)$ + $C_2H_3(^2A')$ and $CH(^2\Pi)$ + C_2H_2 ($^1\Sigma_g^+$) Reactions and Photodissociation of $H_2CC{=}CH(^2B_1)$ at 193 and 242 nm: An Ab Initio/RRKM Study. *J. Phys. Chem. A* **2001**, *105*, 11549−11559.
(64) Chang, A. H. H.; Mebel, A. M.; Yang, X. M.; Lin, S. H.; Lee, Y. T. Ab Initio/RRKM Approach toward the Understanding of Ethylene Photodissociation. *J. Chem. Phys.* **1998**, *109*, 2748−2761.
(65) Miller, W. B.; Safron, S. A.; Herschbach, D. R. Exchange Reactions of Alkali Atoms with Alkali Halides. Collision Complex Mechanism. *Discuss. Faraday Soc.* **1967**, *44*, 108−122.
(66) Kaiser, R. I.; Mebel, A. M. The Reactivity of Ground-State Carbon Atoms with Unsaturated Hydrocarbons in Combustion Flames and in the Interstellar Medium. *Int. Rev. Phys. Chem.* **2002**, *21*, 307−356.